ROSAT Observations of X-ray Emissions from Jupiter During the Impact of Comet Shoemaker-Levy 9

J. H. Waite Jr.,* G. R. Gladstone, K. Franke, W. S. Lewis, A. C. Fabian, W. N. Brandt, C. Na, F. Haberl, J. T. Clarke, K. C. Hurley, M. Sommer, S. Bolton

Röntgensatellit (ROSAT) observations made shortly before and during the collision of comet Shoemaker-Levy 9 with Jupiter show enhanced x-ray emissions from the planet's northern high latitudes. These emissions, which occur at System III longitudes where intensity enhancements have previously been observed in Jupiter's ultraviolet aurora, appear to be associated with the comet fragment impacts in Jupiter's southern hemisphere and may represent brightenings of the jovian x-ray aurora caused either by the fragment impacts themselves or by the passage of the fragments and associated dust clouds through Jupiter's inner magnetosphere.

Auroral x-ray emissions from Jupiter's high magnetic latitudes have been reported in previous studies (*1*, *2*). Although the identity of the particles responsible for these emissions has not been conclusively established, the evidence favors sulfur and oxygen ions originating in the Io plasma torus and accelerated in the outer jovian magnetosphere (*1*, *2*). Auroral ion precipitation is believed to result from pitch angle scattering into the loss cone as the accelerated ions diffuse inward (*3*). In this report we present recent observations made with the ROSAT high-resolution imager (HRI) of intense x-ray emissions from Jupiter's high northern latitudes. These emissions appear to be associated with the impact of fragments of comet Shoemaker-Levy 9 and probably represent a brightening of the jovian x-ray aurora caused either by the impacts themselves or by the passage of the fragments and the associated dust cloud through the inner magnetosphere.

The fragments of Shoemaker-Levy 9 plunged into Jupiter's upper atmosphere at about −40° latitude during the period 16 to 22 July 1994. On 13, 14, and 15 July, the ROSAT HRI acquired preimpact data for comparison with observations made during the impacts. Additional data were acquired from 18 to 22 July, during or near the times of the impacts of fragments K, P, R, S, and W. The x-ray photons were individually detected and time-tagged, allowing us to compensate for the motion of both Jupiter and the ROSAT spacecraft during the observation period and to synthesize images of Jupiter (*4*).

To identify variations associated with the impacts, we created a light curve (Fig. 1) by extracting a small (70 arc sec by 70 arc sec) field centered on the disk of Jupiter from the larger HRI field of view (40 arc min by 40 arc min). Photons arriving in the small field of view were summed over each ROSAT orbit and divided by the corresponding exposure time (*5*). The light curve shows considerable variability, with a noticeable brightening at the times of the K and P2 impacts (*6*).

We investigated the statistical significance of the photon count rate increases as a function of time by performing two standard statistical tests: a Kolmogorov-Smirnov test and its close derivative, the Kuiper test (*7*). We chose these two tests because they are independent of binning start time and width, which can make Poisson-distributed events appear artificially strong. The test space was the northern auroral zone, which we defined as -15 arc sec $< x < 15$ arc sec and 5 arc sec $< y < 25$ arc sec, where x and y are measured from the center of Jupiter toward decreasing jovian longitude and increasing jovian latitude, respectively. We first compared our preimpact data (29,791 s) for 13 to 15 July with earlier data (12,324 s) from May 1992 (*2*). According to both tests, the likelihood that the two data sets were drawn from the same population is ~50%. We then compared the entire set of data acquired during the impacts (33,267 s) with both our preimpact data and the 1992 data. The probability is less than 5×10^{-5} that the impact data are from the same statistical population as the preimpact data and less than 1% that they are from the same population as the 1992 data. As a further test, we combined the 1992 data and the 1994 preimpact data to create a new baseline data set, with which we compared the data for the K (~2200 s) and P2 impacts (~1900 s). The probability that the K impact data and the new baseline data are from the same distribution is less than 8×10^{-5}, and for the P2 impact data, the probability is less than 2×10^{-5}. The results of our analysis indicate that the high count rates detected by HRI during the impact period, particularly near the times of the K and P2 impacts, are unique.

We can examine the timing and intensity of the emission associated with the K impact more closely than is possible in the case of the P2 impact because of the relative intensity of the K impact–associated emission and the availability of correlative data on the K impact from Galileo and both ground-based and Earth-orbiting observatories. In the high-resolution light curve shown in Fig. 2, the x-ray burst occurs at 10:21:25 UT, at approximately the same time as the detection by ground-based observers in Australia of faint emissions at 2.34 μm from the K impact site (10:21:13 UT) (*8*). The infrared emissions are first seen in a frame at 10:20:25 to 10:20:57 UT with a faint precursor event that brightens slightly in the following three frames between 10:21:13 and 10:23:19 UT and then

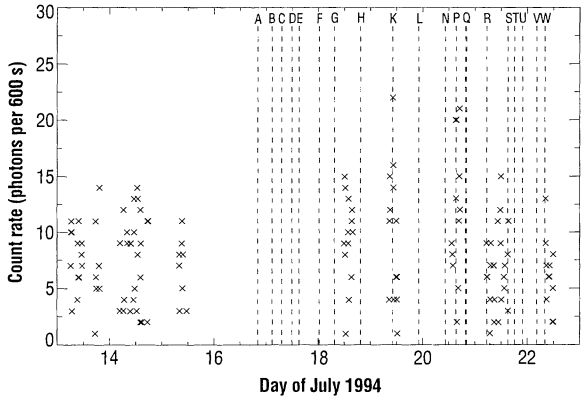

Fig. 1. The ROSAT x-ray light curve for a 70 arc sec by 70 arc sec region centered on Jupiter. The crosses indicate the average count rates from the region during each orbit of Jupiter observations in July 1994. The comet fragment impact times are indicated with vertical dashed lines.

J. H. Waite Jr., G. R. Gladstone, K. Franke, W. S. Lewis, C. Na, Department of Space Science, Southwest Research Institute, P.O. Box 28510, San Antonio, TX 77228–0510, USA.
A. C. Fabian and W. N. Brandt, Institute of Astronomy, University of Cambridge, Cambridge CB3 0HA, UK.
F. Haberl and M. Sommer, Max-Planck-Institut für extraterrestrische Physik, Postfach 1603, D-85740 Garching, Germany.
J. T. Clarke, Space Physics Research Laboratory, University of Michigan, Ann Arbor, MI 48109, USA.
K. C. Hurley, Space Sciences Laboratory, University of California, Berkeley, CA 94720, USA.
S. Bolton, Jet Propulsion Laboratory, Pasadena, CA 91109, USA.
*To whom correspondence should be addressed.

brightens considerably after 10:23:35 UT. Interestingly, both the x-ray and 2.34-μm emissions began about 3 min before the detection, at 0.89 μm, of the K fragment fireball by the Galileo Solid State Imager (SSI). The SSI data for the K impact show that the event began at 10:24:13 UT and lasted about 52 s (9). The 3-min difference in time of observation between the beginning of the x-ray burst and the 2.34-μm precursor, on the one hand, and the flash observed by the SSI, on the other, has not been explained. For our analysis, we define the K impact x-ray event as the eight photons detected over the 220-s interval between the beginning of the x-ray burst at 10:21:25 UT and the end of the flash observed by Galileo.

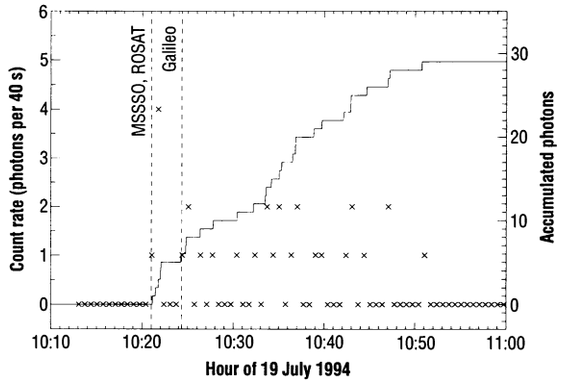

Fig. 2. High-resolution ROSAT x-ray light curve for the K impact. The crosses indicate the number of photons detected in each 40-s interval, and the solid line shows the accumulated photon count from the beginning of the observation period (corresponding to scale on the right). The observed event times for ROSAT, the precursor 2.34-μm signal seen from the Mount Stromlo and Siding Springs Observatory (MSSSO), and the flash seen by the Galileo SSI detector are indicated. The x-ray photons are taken from the northern auroral zone, defined as -15 arc sec $< x <$ 15 arc sec and 5 arc sec $< y <$ 25 arc sec, where x and y are measured from the center of Jupiter toward jovian east and jovian north, respectively.

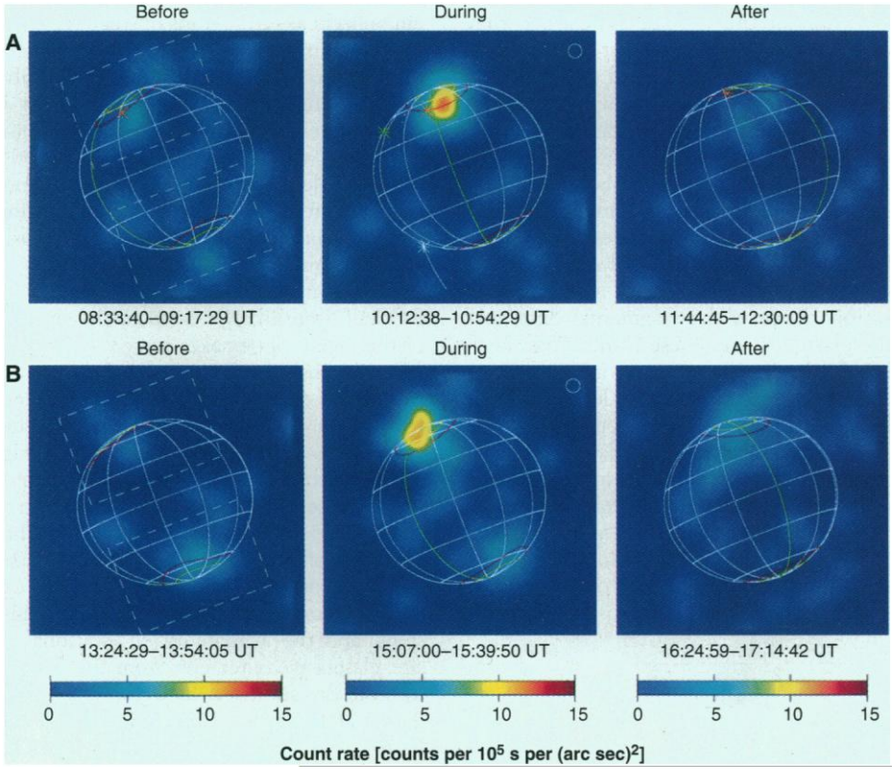

Fig. 3. X-ray images of the signal in a 70 arc sec by 70 arc sec region centered on Jupiter for ROSAT orbits before, during, and after the (**A**) K and (**B**) P2 impacts. The images have been smoothed by the HRI point spread function, and the absolute brightness scale is shown at the bottom. A latitude-longitude grid shows the orientation of Jupiter at the midpoint of each exposure interval (except for the "during" panel of the K impact event, for which the grid represents Jupiter at the impact time). The grid spacings are 30° in both latitude and System III longitude, with the 180° meridian in green. The north and south footprints of the Io plasma torus and the magnetotail region (L = 30) are indicated by the red and yellow lines, respectively. The orange asterisk, when visible, shows the estimated location of the IFT footprint in the northern hemisphere. In the "during" panel for the K impact, the green asterisk shows the magnetic conjugate region to the K impact site, and the trajectory of the K fragment and its position 3 min before impact are shown by a white line and asterisk, respectively. The dashed line boxes in the "before" panels mark the north and south auroral regions used for the statistical studies described in the text. The small (3 arc sec) circle in the upper right corner of the "during" panels represents a conservative estimate of the ROSAT pointing uncertainty.

Figure 3 shows images of Jupiter as seen at x-ray wavelengths before, during, and after both the K and P2 events. To produce these images, data acquired during the observing segments surrounding the K and P2 fragment impacts were smoothed by HRI's point spread function (5). The nominal point spread width is 5 to 6 arc sec, with a comparable nominal uncertainty in pointing; however, the identification and measurement of two stars within the ROSAT field of view during the impact time period make it possible to reduce the pointing uncertainty to less than 3 arc sec (*10*). Given this uncertainty, the brightest x-ray emissions appear to occur near System III longitude λ_{III} = 170° and +50° latitude during the K event, and near longitude λ_{III} = 180° and +70° latitude during the P2 event (the differences in latitude and longitude between the two emission regions are within the 3–arc sec pointing uncertainty of the observations). Interestingly, the K emission peak is located near the foot of the Io flux tube (IFT: λ_{III} = 186°, latitude = +50°), a known source of auroral emissions (*11*). The location of the P2 peak is not as close to the foot of the IFT (IFT: λ_{III} = 273°, latitude = +75°). The occurrence of the K burst near the foot of the IFT may or may not be coincidental and indicative of IFT involvement in the generation of the emissions. In contrast to the transient ultraviolet emissions observed by the Hubble Space Telescope (HST) 45 min after the K impact (*12*), the x-ray emissions associated with the K event do not occur near the northern magnetic conjugate point of the impact site (λ_{III} = 269°, latitude = +38°), as we initially reported (*13*) before our final pointing determination was made.

Observations of the jovian aurora at ultraviolet (UV) and infrared (IR) wavelengths show the aurora to exhibit both rotational and temporal variations in emission intensity (*14*). Although less extensive than the data on the UV and IR auroras, ROSAT x-ray data acquired in 1992 indicate that the x-ray aurora displays a rotational or longitudinal variability consistent with that of the UV and IR aurora, with a peak in emission intensity near the central meridian longitude (CML) range λ_{III} = 180° to 200° (*2*). The fact that the x-ray bursts observed near the times of the K and P2 impacts occur near this longitude range

raises the possibility that HRI simply detected normal, longitude-dependent increases in the intensity of Jupiter's x-ray aurora. To test this possibility, we combined preimpact x-ray data with impact-period data (minus the bright events associated with the K and P2 impacts) to produce a rotational light curve (Fig. 4) and calculated an average peak emission intensity at a CML of λ_{III} = 170° to 180° of 0.006 count per second. We then compared this count rate with that observed in association with the K and P2 events. According to Poisson statistics, the probability is 6×10^{-5} that the 220-s eight-photon burst associated with the K impact was from the rotational light curve of the auroral oval; for the P2 event, the probability is 3×10^{-4}.

Thus, the K and P2 events are statistically different from increases expected of the normal x-ray aurora near CMLs of λ_{III} = 180° to 200°. We cannot, however, rule out the possibility that we observed unusually bright auroral events that occurred only coincidentally near the time of the K impact. Dramatic brightenings of the UV aurora have been observed by HST (*15*), for example, and it is possible that ROSAT detected a similar event at x-ray wavelengths. Although our x-ray data are too limited to permit us to dismiss this possibility, it seems highly unlikely that two such events would both occur coincidentally at or very near the times of fragment impacts. Moreover, observations by the International Ultraviolet Explorer suggest that the UV aurora—and by implication, the x-ray aurora as well—was quiet around the time of the K impact (*16*).

If, as our analysis indicates, the observed x-ray enhancements were indeed correlated with the fragment impacts, by what processes might they have been triggered? Possible emission mechanisms include electron bremsstrahlung or K shell emission from precipitating energetic sulfur and oxygen ions. Both mechanisms have been proposed to explain the auroral x-rays observed previously by the Einstein Observatory and ROSAT (*1*, *2*). Unfortunately, we have no statistically meaningful information from ROSAT about the energy spectra of the x-rays observed in association with the impacts (*17*) and no direct information about the energies of the precipitating particles. Whether ions or electrons, we assume that the fragment impacts did not directly energize the particles responsible for the emissions because of the timing of the x-ray events, but triggered particle precipitation from an existing reservoir of energetic charged particles in Jupiter's inner magnetosphere.

Whatever the particular emission mechanism, the processes responsible for the K and P2 x-ray events may have been triggered either by the impacts themselves or by the passage of the fragments and associated dust through Jupiter's inner magnetosphere. The fact that the x-ray emissions associated with the K event were detected about 3 min before the observation of the fireball by Galileo may indicate that the x-ray burst occurred before the actual impact and suggests that fragment-dust interactions with the inner magnetospheric plasma before impact were responsible for the observed brightening. However, at 3 min before impact, the K fragment was crossing field lines that map to lower latitudes and higher longitudes than those at which the emissions were observed (*18*). If a direct interaction between the fragments, dust, and the plasma within these L shells had been involved, the emissions would have occurred at these lower latitudes and higher longitudes. Instead, they occurred near the auroral zone latitudes and System III longitudes where the emission maxima of the normal UV aurora are also observed (*19*).

On the other hand, the faint precursor emission detected at 2.34-μm at about the same time as the beginning of the K x-ray event suggests an interaction of the fragment or dust with Jupiter's upper atmosphere and ionosphere and thus a process triggered by the impacts themselves. Further, the absence of impact residue at visible wavelengths suggests that the P2 fragment dissipated high in the atmosphere (*20*), favoring a process involving the deposition of energy in the magnetosphere-ionosphere coupling region. Such a process might produce magnetohydrodynamic shocks capable of accelerating trapped radiation belt particles (*21*) or electromagnetic and plasma waves capable of interacting with the electrons and ion populations in the inner magnetosphere.

If the emissions had been caused by an impulsive, impact-induced process, the intensity maxima would likely have been correlated with the minimum in surface magnetic field strength. However, they appear to have occurred near longitudes where the magnetic field is strongest and the field gradients are inferred to be steepest (*22*). In the case of the UV aurora, the emission peaks in regions of steep negative gradients in the magnetic field strength have been attributed to processes involving gradient curvature drift (*19*). Drift is slow, however, requiring 60 jovian rotations for 1-MeV heavy ions to drift 360°, for example. A drift process thus cannot easily be invoked to explain precipitation events that occur nearly simultaneously with the impacts.

The x-ray enhancements observed by ROSAT were likely related to the impacts of the comet Shoemaker-Levy 9 fragments. The fact that the emission peaks were detected in a region where intensity enhancements occur in the normal UV aurora suggests that processes related to the comet fragment impacts caused a significant brightening of Jupiter's x-ray aurora. Identification of these processes, however, must await further synthesis of the data acquired during the comet impacts, the availability of more extensive data on jovian auroral x-ray emissions, and the availability of additional in situ plasma measurements from the Galileo mission. In addition, hard x-ray data acquired at the time of the K impact by the Earth-orbiting Compton Gamma Ray Observatory and the Solar X-ray/Cosmic Gamma Ray Burst Detector on the Ulysses spacecraft are being analyzed.

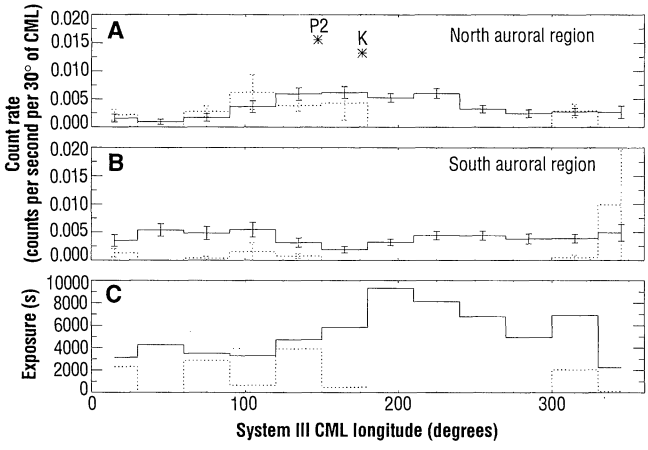

Fig. 4. (**A** and **B**) Rotational x-ray light curves for Jupiter. The solid line histogram and error bars show the ROSAT count rates averaged in 30° bins of central meridian longitude (CML), using all the July 1994 data except the orbits containing the K and P2 impacts, which are shown individually as asterisks. The dotted line histogram and error bars are from the May 1992 ROSAT data (*2*). The (A) north and (B) south auroral regions from which the data were taken are defined in Fig. 3. (**C**) The total exposure time acquired in each 30° CML bin.

REFERENCES AND NOTES

1. A. E. Metzger *et al.*, *J. Geophys. Res.* **88**, 7731 (1983).
2. J. H. Waite Jr. *et al.*, *ibid.* **99**, 14799 (1994).
3. N. Gehrels and E. Stone, *ibid.* **88**, 5537 (1983).
4. Details of this method are presented in (*2*).
5. L. P. David, F. R. Harnden Jr., K. E. Kearns, M. V. Zombeck, in *The ROSAT High Resolution Imager* (U.S. ROSAT Science Data Center and Smithsonian Astrophysical Observatory, Cambridge, MA, 1995).

Counts with pulse height analyzer channel numbers <4 (out of a 1 to 16 range) were eliminated to avoid contamination from UV emissions.
6. The x-ray emissions observed in association with the K and P2 impacts appear to display a longitude dependence similar to that of the UV aurora and to that postulated for the normal x-ray aurora (*2*). The longitude region within which they occurred was not visible to ROSAT at the times of the R and S fragment impacts, however, which may explain why no enhanced counts were detected in association with these events. ROSAT may have detected a weak signature near the time of the W impact; however, data collection did not start until about 6 min after the W impact. The relatively weak W signature may represent the waning tail of a more active x-ray emission period.
7. The Kolmogorov-Smirnov and Kuiper tests used in our analysis of the K and P2 observations are described in W. H. Press, S. A. Teukolsky, W. T. Vetterling, B. P. Flannery, *Numerical Recipes in FORTRAN: The Art of Scientific Computing* (Cambridge Univ. Press, Cambridge, ed. 2, 1992), pp. 617–622. Although we used both tests, we cite only the Kuiper statistics, which are more conservative (generally by a factor of 10) than the Kolmogorov-Smirnov statistics.
8. Information about the 2.34-μm observations made at the Australian National University's Mount Stromlo and Siding Springs Observatory was kindly provided by P. McGregor, personal communication.
9. C. R. Chapman *et al.*, *Geophys. Res. Lett.*, in press.
10. ROSAT's normal pointing uncertainty of 5 arc sec (1σ) was considerably improved upon for our Jupiter observations by the fortuitous presence of two astrophysical x-ray point sources within the 40–arc min–diameter field of view. High-precision positions for the optical counterparts to the two sources near the time of the impacts were kindly provided to us by O. A. Naranjo (personal communication). One of the sources is at right ascension (RA) 14 hours, 13 min, and 5.14 s and declination (DEC) 12°, 1 arc min, and 24.4 arc séc and is identified as the star GQ Vir. The other source is at RA 14 hours, 12 min, and 39.1 s and DEC 12°, 9 arc min, and 10.8 arc sec and is unidentified in the visible. Using these positions, we corrected the ROSAT data by shifting the centroided counts from these two sources to the above positions. The final pointing accuracy appears to be good to within ±1.5 arc sec.
11. J. E. P. Connerney, R. Baron, T. Satoh, T. Owen, *Science* **262**, 1035 (1993).
12. J. T. Clarke *et al.*, *ibid.* **267**, 1302 (1995).
13. J. H. Waite *et al.*, *Eos* **74** (suppl.), 404 (1 November 1994).
14. For data on the variability in the brightness of the UV and IR auroras, see T. A. Livengood, thesis, Johns Hopkins University (1991) and H. A. Lam, thesis, University College, London (1995).
15. J. C. Gérard *et al.*, *Science* **266**, 1675 (1994).
16. W. M. Harris *et al.*, in preparation; J. T. Clarke *et al.*, *Bull. Am. Astron. Soc.* **26**, 1100 (1994).
17. ROSAT's Position Sensitive Proportional Counter (PSPC) determines with a $\Delta E/E$ of 30% the energy E of incident x-ray photons over an energy range 0.12 to 2.1 keV. Unfortunately, PSPC observations were not made during the impact period. Limited inferences about particle energy can be made, however, on the basis of the ratios of HRI's low-energy pulse height analyzer (PHA) channels (4 to 5) to the higher energy channels (6 to 8) (*5*). The PHA ratio for the preimpact observations was 3.5 ± 0.9; the ratio for the x-rays detected during the 42 min surrounding the K event was 2.4 ± 1.6.
18. J. E. P. Connerney, private communication. The K fragment trajectory in Jupiter's magnetosphere was calculated with the Goddard Space Flight Center O6 magnetic field model and magnetodisc model [J. E. P. Connerney, M. H. Acuña, N. F. Ness, *J. Geophys. Res.* **86**, 8370 (1981); J. E. P. Connerney, *ibid.* **98**, 18659 (1993)].
19. F. Herbert, B. R. Sandel, A. L. Broadfoot, *ibid.* **92**, 3141 (1987).
20. H. B. Hammel *et al.*, *Science* **267**, 1288 (1995).
21. S. H. Brecht, M. Pesses, J. G. Lyon, N. T. Gladd, S. W. McDonald, *Geophys. Res. Lett.*, in press.
22. See (*19*) and references therein.

23. We thank S. H. Brecht, I. de Pater, and A. J. Dessler for sharing unpublished results and for valuable discussions; O. A. Naranjo and N. Schneider for information relevant to pointing issues; D. Glicksberg for data on the K fragment trajectory; J. E. P. Connerney for plotting the K fragment trajectory across Jupiter's magnetic field lines; and G. J. Fishman and B. C. Rubin for the Compton Gamma Ray Observatory BATSE (Burst and Transient Source Experiment) data. We gratefully acknowledge the work of the ROSAT team. ROSAT is supported by the Bundesministerium für Forschung und Technologie. J.H.W. acknowledges support from the ROSAT Guest Observer Program (NAG5-2617) and from the National Aeronautics and Space Administration Planetary Atmospheres program (NAGW-3624). A.C.F. thanks the Royal Society, and W.N.B. thanks the National Science Foundation and the British Overseas Research Studentship Programme for financial support.

18 October 1994; accepted 7 April 1995

Microchronology and Demographic Evidence Relating to the Size of Pre-Columbian North American Indian Populations

Dean R. Snow

Recent estimates for the size of the aggregate North American Indian population in A.D. 1492 vary from about 18 million to less than 2 million. The unusually favorable archaeological characteristics of Mohawk Iroquois sites in eastern New York have allowed a detailed demographic reconstruction of one case for the period A.D. 1400 to 1776. The case indicates that exogenous epidemics did not reach the region until the 17th century and supports arguments favoring the lower populations estimates for North America as a whole.

The sizes of pre-Columbian populations in the Americas have been the subjects of scholarly debate in recent years (*1*). The debate has been prompted mainly by the hypothesis that unrecorded exogenous pandemics reduced American Indian populations by very large fractions during the 16th century (*2*). The hypothesis presumes that the earliest population estimates available from documentary sources for North American Indian populations are, more often than not, postepidemic counts, and that numbers must have been higher prior to A.D. 1492. How much higher depends on the severity and ubiquity of the pandemics presumed to have occurred between A.D. 1492 and the earliest available counts (*3*).

A remnant population of 2000 implies a preepidemic population of 10,000 if 80% mortality is assumed, but the reconstructed initial figure is twice that size if the mortality rate is raised by only another 10%. Thus, for North America alone, one scholar puts the estimate at 18 million for A.D. 1492, whereas several others argue for a figure about a tenth that size (*2*, *4*, *5*).

There is no evidence for exogenous pandemics in northeastern North America before A.D. 1616, even though they began a century earlier in areas of Spanish settlement around the Caribbean (*6*). Two of the reasons for the lag appear to be the quarantine effects of small crew sizes and long crossing times before A.D. 1600. However, the most important factor was the absence of children in parties of Europeans making contact with American Indians outside the sphere of Spanish colonization. Smallpox and the other exogenous epidemics that devastated American Indian populations were childhood diseases in Europe at the time; nearly all European adults were survivors of these childhood illnesses who enjoyed lifelong immunity and were not contagious to the susceptibles they might contact. The Spanish brought children with them early, with devastating effects. Children did not accompany French, Dutch, and English colonists until much later.

If timing was important, so too was the ubiquity of diseases. Although it is an essential component of any scenario involving dramatic widespread population declines in the 16th century, it has not been demonstrated that every epidemic became a continent-wide pandemic. The available evidence is more consistent with patterns of local and regional epidemics that affected some parts of the continent decades (sometimes centuries) before others (*4*, *5*).

The Mohawk Indian nation was and is one of the constituent nations of the League of the Iroquois. Data from the Mohawk archaeological site sequence in New York State provide support for the lower current estimates of pre-Columbian population sizes (Fig. 1). The Mohawks practiced a northern swidden form of horticulture that entailed village relocations every decade or two. Mohawk villages were compact, usually palisaded, and regular in their construc-

Department of Anthropology, University at Albany, State University of New York, Albany, NY 12222, USA.